27

Investigation on Oblique Shock Wave Control by Surface Arc Discharge in a Mach 2.2 Supersonic Wind Tunnel

Yinghong Li[1] and Jian Wang[2]
[1]*Engineering College, Air Force Engineering University*
[2]*Army Aviation Institute*
China

1. Introduction

A shock wave is a typical aerodynamic phenomenon in a supersonic flow, and if controlled effectively, a series of potential applications can be achieved in aerospace fields, such as reducing wave drag and sonic boom of the supersonic vehicle, optimizing shock waves of the supersonic inlet in off-design operation states, decreasing pressure loss induced by shock waves in the supersonic wind tunnel or aeroengine internal duct, controlling shock waves of the wave rider, changing shock wave symmetry to achieve flight control and inducing shock waves in the aeroengine nozzle to achieve thrust vector control.

Shock wave control can be achieved by many mechanical or gas dynamic methods, such as the ramp angle control in supersonic inlet and the holl/cavum control in self-adapted transonic wing. Because the structural configurations of these methods are somewhat complex and the flow control response is also slow, plasma flow control based on gas discharge physics and electromagnetohydrodynamics (EMHD) theory has been developed recently in the shock wave control field. Using this method, substantial thermal energy can be added in the shock wave adjacent areas, then the angle and intensity of shock wave change subsequently.

Meyer *et al* investigated whether shock wave control by plasma aerodynamic actuation is a thermal mechanism or an ionization mechanism, and the experimental results demonstrated that the thermal mechanism dominates the shock wave control process [1, 2]. Miles *et al* investigated the shock wave control by laser energy addition experimentally and numerically, and the research results showed that when the oblique shock wave passed by the thermal spot induced by laser ionization, the shock wave shape distorted and the shock wave intensity reduced [3]. Macheret *et al* proposed a new method of virtual cowl induced by plasma flow control which can optimize the shock waves of supersonic inlet when its operation Mach number is lower than the design Mach number [4]. Meanwhile, they used the combination method of e-beam ionization and magnetohydrodynamic (MHD) flow control to optimize the shock waves of supersonic inlet when operating in off-design states, and the research results demonstrated that the shock waves can reintersect in the cowl adjacent area in different off-design operation states with the MHD acceleration method and the MHD power generation method, respectively [5]. Leonov *et al* used a quasi-dc

filamentary electrical discharge, and the experimental results showed that shock wave induction, shock wave angle transformation and shock wave intensity reduction, etc could all be achieved by plasma flow control [6-8]. Other than oblique shock wave control, the bow shock wave control by plasma aerodynamic actuation was also studied by Kolesnichenko *et al* [9], Ganiev *et al* [10], and Shang *et al* [11] for the purpose of reducing peak thermal load and wave drag.

This paper used the arc discharge plasma aerodynamic actuation, and the wedge oblique shock wave control by this plasma aerodynamic actuation method was investigated in a small-scale short-duration supersonic wind tunnel. The change laws of shock wave control by plasma aerodynamic actuation were obtained in the experiments. Moreover, a magnetic field was applied to enhance the plasma actuation effects on a shock wave. Finally, a qualitative physical model was proposed to explain the mechanism of shock wave control by plasma aerodynamic actuation in a cold supersonic flow.

2. Experimental setup

The design Mach number of the small-scale short-duration supersonic wind tunnel is 2.2 and its steady operation time is about 30-60 s. The test section is rectangular with a width of 80mm and a height of 30 mm. The gas static pressure and static temperature in the test section are 0.5 atm and 152 K, respectively. The groove in the test section lower wall is designed for the plasma aerodynamic actuator fabrication.

The power supply consists of a high-voltage pulse circuit and a high-voltage dc circuit. The output voltage of the pulse circuit can reach 90 kV, which is used for electrical breakdown of the gas. The dc circuit is the 3 kV-4 kW power source, which is used to ignite the arc discharge.

The plasma aerodynamic actuator consists of graphite electrodes and boron-nitride (BN) ceramic dielectric material. Three pairs of graphite electrodes are designed with the cathode-anode interval of 5mm and the individual electrode is designed as a cylindrical structure which is embedded in the BN ceramic. The upper gas flow surface of electrodes and ceramic must be a plate to ensure no unintentional shock wave generation in the test section. The controlled oblique shock wave is generated by a wedge with an angle of 20°. As shown in figure 1, the plasma aerodynamic actuator is embedded in poly-methyl-methacrylate (PMMA) and then inserted into the groove of the test section lower wall. There are 10 pressure dots with a diameter of 0.5mm along the flow direction for the gas pressure measurement.

As shown in figure 2, the static magnetic field is generated by a rubidium-iron-boron magnet which consists of four pieces. Two pieces construct the N pole and the other two pieces construct the S pole. The magnetic field strength in the zone of interaction is about 0.4 T. Based on the MHD theory, the main purpose of adding magnetic field is applying a Lorentz body force to the charged particles in the arc plasma, which can influence the plasma actuation effects on shock wave.

The test systems consist of a gas pressure measurement system, a schlieren photography system and an arc discharge voltage-current measurement system. The gas pressure measurement system is used to measure and compute the oblique shock wave intensity with the data-acquisition frequency of 1 kHz and the acquisition time of 3-10 s. The schlieren photography system is used to photograph the configuration of the oblique shock wave. It uses the Optronis® high-speed CCD camera with the maximum framing rate of 200 000 Hz.

For the purpose of acquiring the pulsed arc discharge process in the flow, the framing rate in this paper is selected as 8000 Hz with an exposure time of 0.0001 s and a resolution of 512 × 218 pixels. The arc discharge voltage and current are monitored by a voltage probe (P6015A, Tektronix Inc.) and a current probe with a signal amplifier (TCP312+TCPA300, Tektronix Inc.), respectively. The two signals are measured by a four-channel digital oscilloscope (TDS4104, Tektronix Inc.).

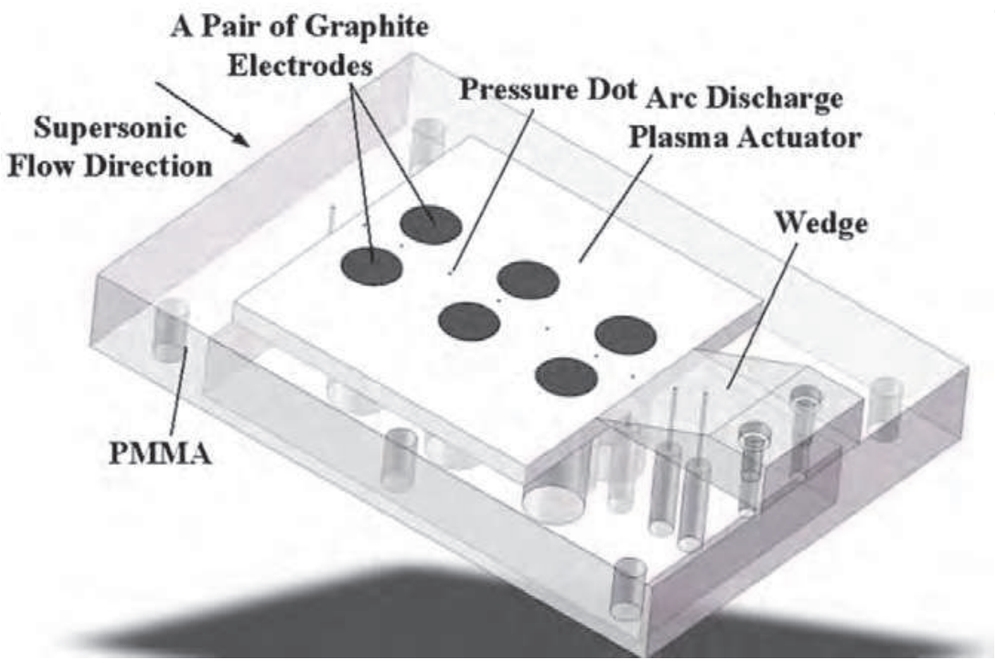

Fig. 1. Sketch of arc discharge plasma aerodynamic actuator.

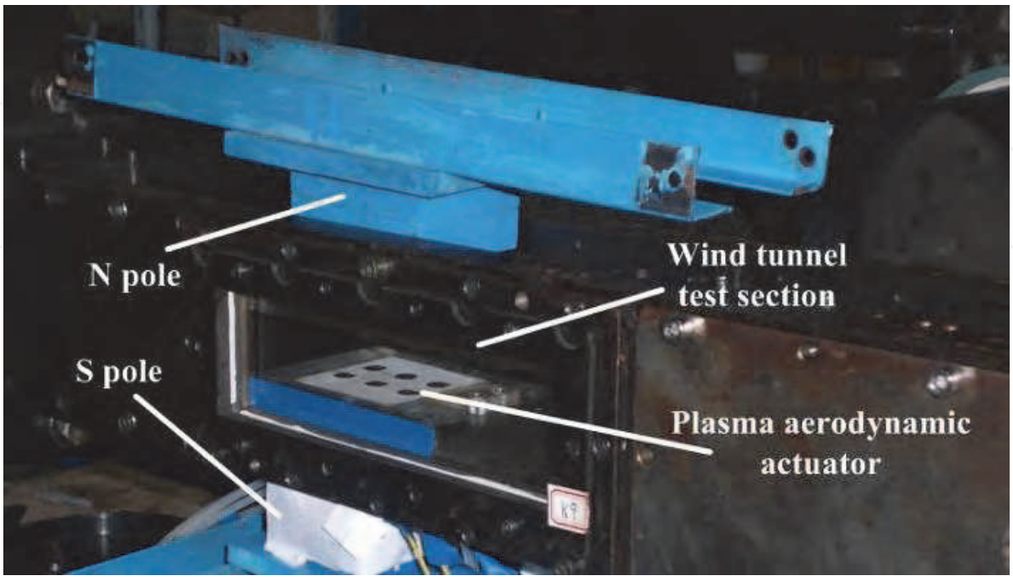

Fig. 2. Sketch of magnet fabrication on the wind tunnel test section.

3. Test results and discussion

3.1 Electrical characteristics

Under the test conditions of Mach 2.2, the arc discharge is a pulsed periodical process with a period of 2-3 ms, and the discharge time only occupies 1/20 approximately in a period. The discharge voltage-current curves including several discharge periods are shown in figure 4(a). It can be seen that the discharge intensity is unsteady with some periods strong but some other periods weak. The discharge voltage-current-power curves in a single period are shown in figure 4(b). The discharge process in a single period can be divided into three steps. The first step is the pulse breakdown process. When the gas breakdown takes place, the discharge voltage and the current can reach as high as 13 kV and 18 A, respectively, and the discharge power reaches hundreds of kilowatts. However, this step lasts for an extremely short time of about 1 μ s, which indicates that it is a typical strong pulse breakdown process. The second step is the dc hold-up process. After the pulse breakdown process, arc discharge starts immediately. The discharge voltage decreases from 3 kV to 300-500V and the discharge current increases to 3-3.5A correspondingly. The discharge power is maintained at 1-1.5 kW. This step lasts for a long time of about 80 μ s. The third step is the discharge attenuation process. Because the supersonic flow blows the plasma channel of the arc discharge downstream strongly, the Joule heating energy provided by the power supply dissipates in the surrounding gas flow intensively. As a result, the discharge voltage increases gradually. Both the discharge current and power decrease. When the power supply cannot provide the discharge voltage, the discharge extinguishes. After some time, the next period of discharge will start again. This attenuation step lasts for about 20 μ s. The time-averaged discharge power of the above three steps within 100 μ s is about 1.3kW.

From figure 3 we can see that the arc discharge plasma is strongly bounded near the wall surface and blown downstream by the supersonic flow. The arc discharge is transformed from a large-volume discharge under static atmospheric conditions to a large-surface discharge under supersonic flow conditions.

Fig. 3. Arc discharge picture in the supersonic flow.

3.2 The wedge oblique shock wave control by typical plasma aerodynamic actuation

Three pairs of electrodes discharge simultaneously in the experiments. Under the conditions of an input voltage of 3 kV and an upwind-direction magnetic control, the wedge oblique shock wave control by this plasma aerodynamic actuation was investigated in detail. Because of the fabrication error and actuator surface roughness, there are some unintentional shock waves in the test section before the wedge. The wedge in the supersonic flow generates a strong oblique shock wave, which can be seen from figure 5(a). Because the boundary layer in the test section lower wall before the wedge is somewhat thick with a thickness of about 3-4 mm, the start segment of the oblique shock wave is composed of many weak compression waves, which intersect in the main flow to form the strong oblique shock wave.

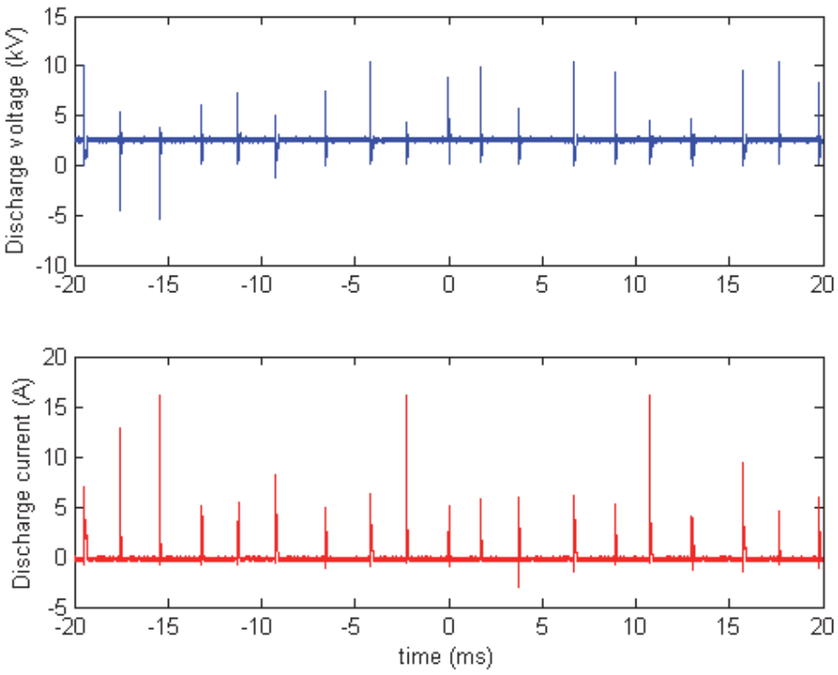

(a)

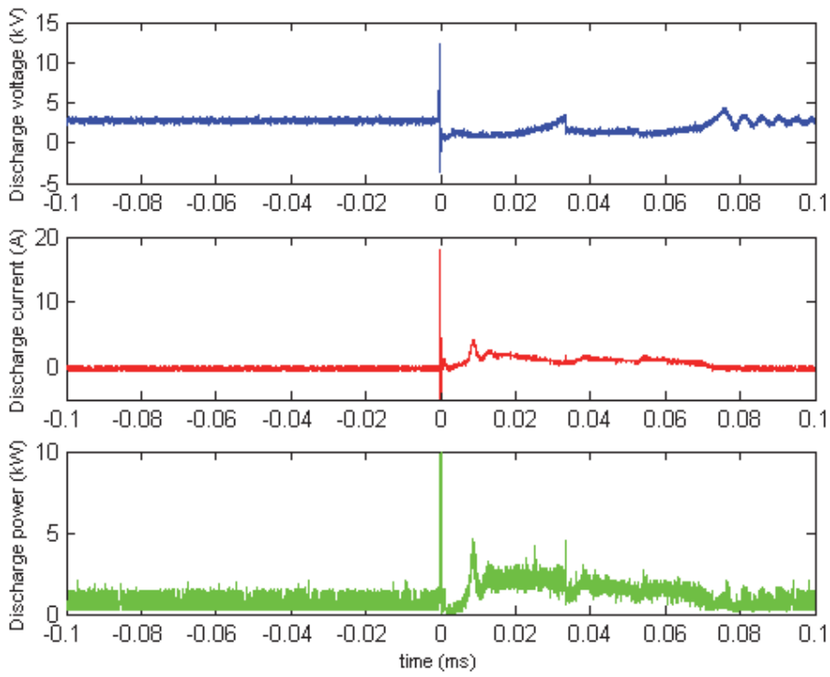

(b)

Fig. 4. Electrical characteristics of arc discharge in supersonic flow. (a) Discharge voltage-current curves including several discharge periods. (b) Discharge voltage-current-power curves in a single period.

When applying plasma aerodynamic actuation, the schlieren test results showed that the structure of the wedge oblique shock wave changed distinctly. Within the discharge time, the intensity of the shock wave change was from weak to strong and then to weak again, which indicated that the shock wave control was a dynamic process, which was consistent with the unsteady characteristics of the three discharge steps discussed in section 3.1. However, within the extinction time, the shock wave recovered to the undisturbed state as before, which demonstrated that the arc discharge control on shock wave was a pulsed periodical process. The mostly strong shock wave control effect within the discharge time is shown in figure 5(b). We can see that the start segment of the wedge oblique shock wave is transformed from a narrow strong wave to a series of wide weak waves, and the start point of the shock wave shifts 4mm upstream, its angle decreases from 35° to 32° absolutely and 8.6% relatively, and its intensity weakens as well. This phenomenon is somewhat similar to the supersonic inlet design method of transforming a strong shock wave to a series of weak shock waves for the purpose of reducing flow pressure loss.

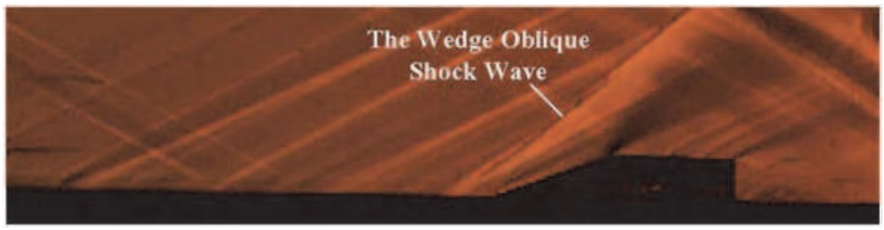

(a)

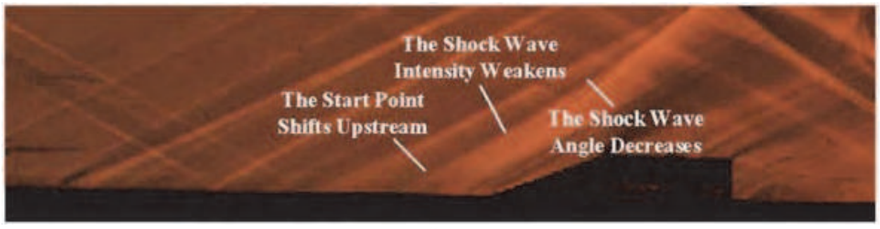

(b)

Fig. 5. Influence of plasma aerodynamic actuation on the structure of wedge oblique shock wave. (a) Schlieren picture without plasma aerodynamic actuation. (b) Schlieren picture with plasma aerodynamic actuation.

Confined by the upper limit 1 kHz of data-acquisition frequency, the pressure measurement system cannot precisely distinguish the pulsed process of shock wave control, so the pressure data in this paper are just the macro time-averaged description of plasma flow control on shock wave. The intensity of wedge oblique shock wave is defined as the pressure ratio of shock wave downstream flow (pressure dot 10) on shock wave upstream flow (pressure dot 7). Because of flow turbulence and unsteadiness in the wind tunnel test section, the pressure data have a little fluctuation with the intensity less than 1%. As seen from figure 6, when applying plasma aerodynamic actuation, the shock wave intensity greatly decreases with the time-averaged intensity from 2.40 to 2.19 absolutely and 8.8% relatively. Hence, we can conclude that the plasma aerodynamic actuation controls the wedge oblique shock wave effectively.

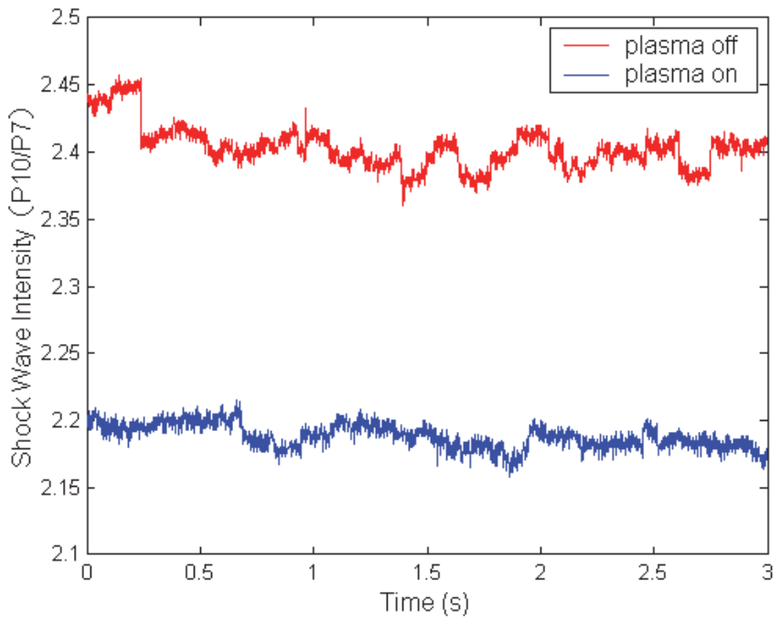

Fig. 6. Influence of plasma aerodynamic actuation on the intensity of wedge oblique shock wave.

3.3 Magnetic control on shock wave

The basic principle of magnetic control is applying the Lorentz body force to the arc discharge current. The mathematical expression is $\vec{F} = \vec{j} \times \vec{B}$, where $\vec{j}$ refers to the discharge current density vector, $\vec{B}$ refers to the magnetic field intensity vector and $\vec{F}$ refers to the Lorentz body force vector. By changing the direction of the discharge current, both the upwind-direction and the downwind-direction Lorentz force can be achieved, as shown in figure 7.

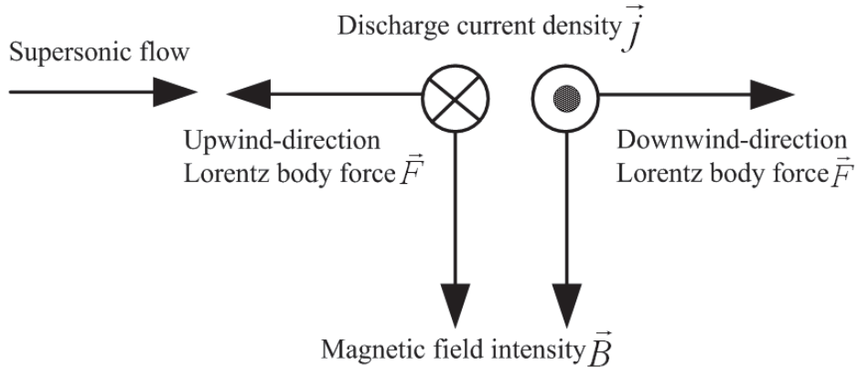

Fig. 7. Basic principle of magnetic control on gas discharge.

From the shock wave intensity measurements in figure 8, we can see that magnetic control greatly intensifies the shock wave control effects. When applying plasma aerodynamic actuation without magnetic control, the intensity of the wedge oblique shock wave

decreases only by 1.5%, but when applying the upwind-direction magnetic control, it decreases by 8.8%. Moreover, when applying the downwind-direction magnetic control, it decreases by 11.6%. The experimental results showed that the maximum shock wave intensity decrease is 20.2%. Hence we can conclude that magnetic control greatly intensifies the shock wave control effects and the downwind-direction magnetic control is better than the upwind-direction magnetic control.

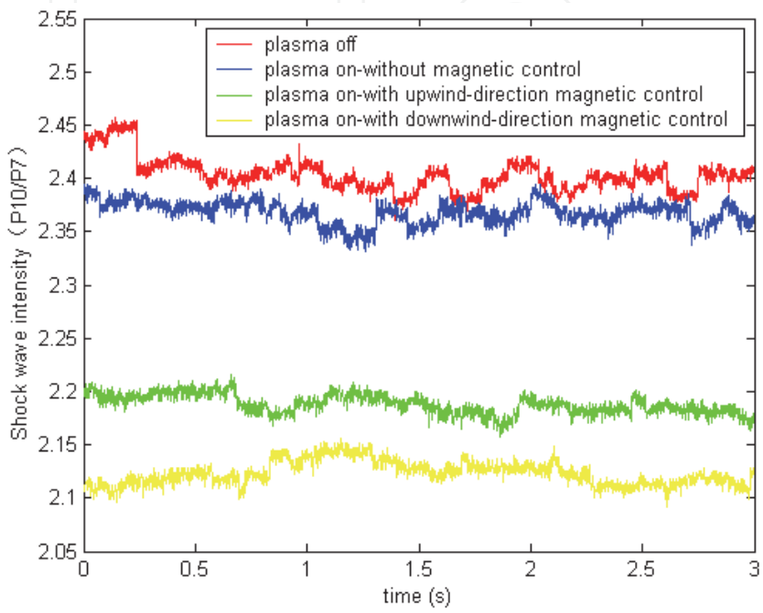

Fig. 8. Influence of magnetic control on shock wave intensity.

Then the mechanism of enhancement of plasma actuation effects on the shock wave by magnetic field is discussed. The discharge characteristics without or with magnetic field under the conditions of no flow are measured and the results demonstrate that they are very different. The voltage, current and power measurements without magnetic field are shown in figure 9. The gas breakdown voltage between the graphite electrodes is about 2 kV and when the input voltage provided by the power supply exceeds this value, arc discharge happens. At the instant of gas breakdown, voltage decreases from 2 kV to about 300 V and current increases to about 1 A. The discharge power is calculated as 300 W. Then the voltage holds at 300 V, but the current decreases gradually. After about 0.5 s, the current sustains at about 440 mA and the discharge power holds at about 130 W. Until now, the steady state of arc discharge is achieved. The above discharge characteristics demonstrate that the arc discharge without magnetic field can be separated into two phases, which correspond to the strong pulsed breakdown process and the steady discharge process, respectively.

When the magnetic field is applied, the discharge characteristics are shown in figure 10 and we can see that the arc discharge transitions from the continuous mode to the pulsed periodical mode. The discharge period is very unstable from tens of milliseconds to several seconds. In a typical discharge period, the discharge time only occupies several milliseconds, which demonstrates that the discharge extinguishes within most time of a period. At the instant of pulsed discharge, voltage decreases to about 500 V and current increases to about 1.2 A. The discharge power is calculated to be about 600 W. These discharge characteristics with magnetic field are very similar to the conditions in the flow

and show great differences under the conditions without the magnetic field. Two remarkable differences are concluded.

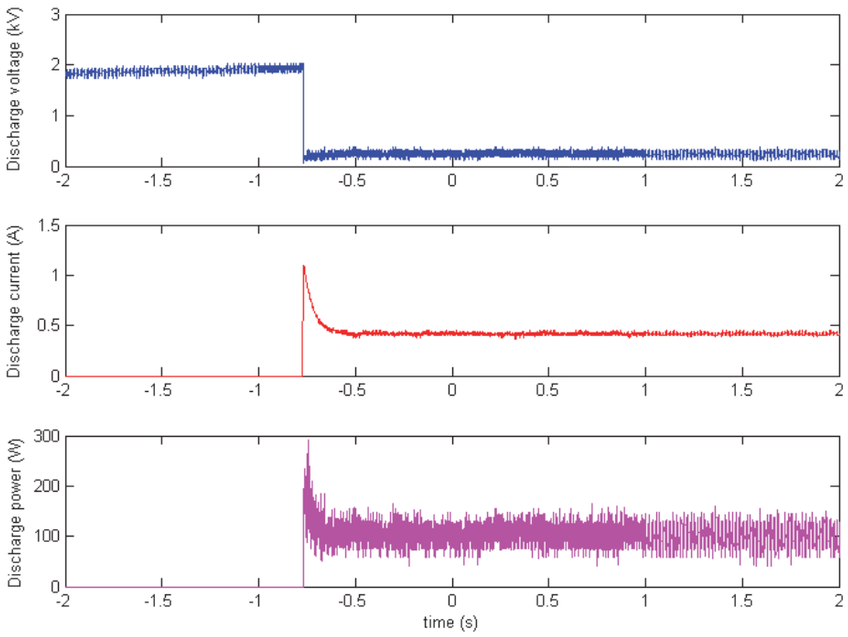

Fig. 9. Electrical characteristics of arc discharge under the conditions of no magnetic field and no flow.

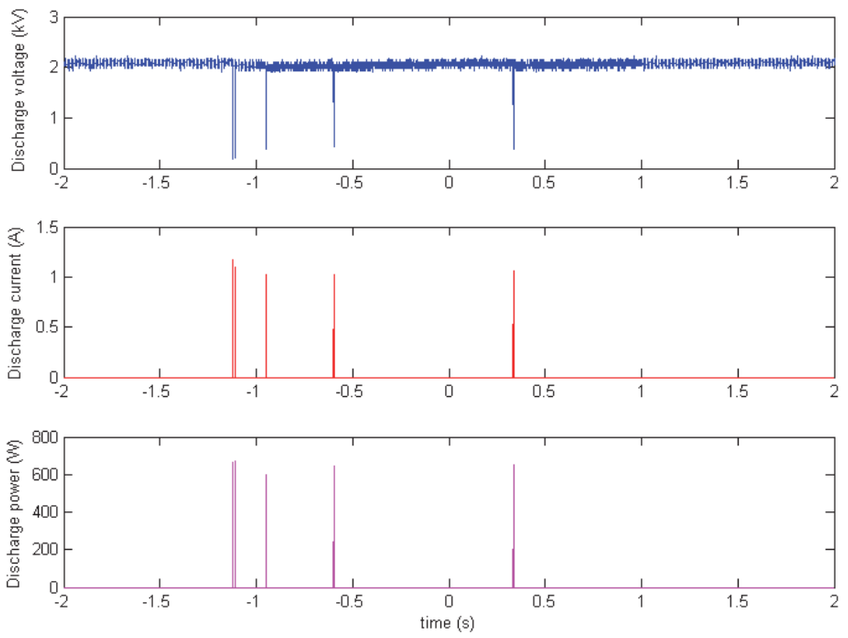

Fig. 10. Electrical characteristics of arc discharge under the conditions of magnetic field and no flow.

Firstly, the arc discharge transitions from the continuous mode to the pulsed periodical mode. When the arc discharge reaches the steady state, the Joule heating energy provided by the power supply must balance the dissipated energy, such as convection loss, conduction loss and radiation loss. Under the conditions of no magnetic field and no flow, convection loss mainly refers to the energy loss of natural convection process that the hot arc plasma transfers thermal energy to the cold surrounding air. Conduction loss mainly refers that the hot arc plasma transfers the thermal energy to the cold electrodes and the ceramic surfaces. As the Joule heating energy can balance the dissipated energy, the arc discharge can reach the steady state. However, under the condition of magnetic field, the plasma channel of the arc discharge is greatly deflected by the Lorentz body force, which is shown in figure 11. Besides the natural convection process, the arc plasma also endures intensive constrained convection process, which dissipates the Joule heating energy substantially. Therefore, the Joule heating energy provided by the power supply cannot balance the dissipated energy, so the discharge extinguishes quickly.

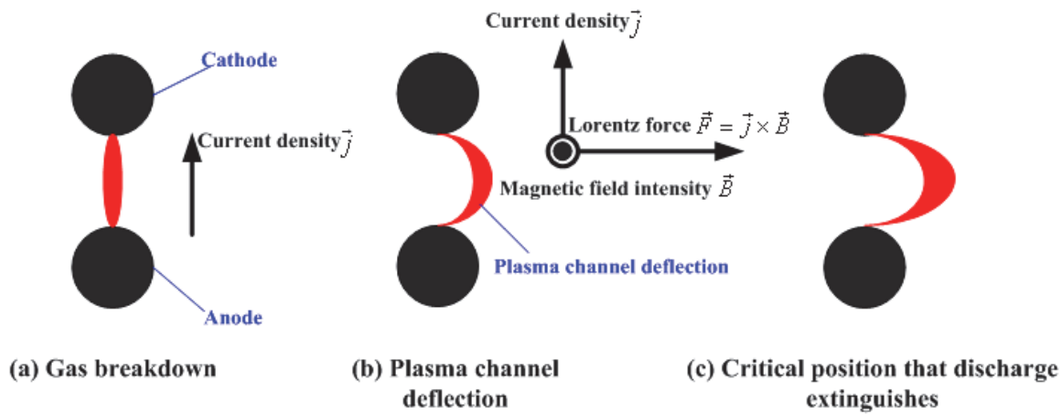

Fig. 11. Sketch of plasma channel deflection by Lorentz force under the condition of magnetic field.

Secondly, the discharge power increases. At the instant of gas breakdown, the power deposition by the arc discharge increases from 300 to 600 W under the condition of magnetic field. So we can deduce the preliminary fact that the power deposition in the flow also increases after the application of the magnetic field. Therefore, the shock wave control effect is intensified by the magnetic field as measured in the experiments. So we suppose that the observed enhancement of discharge effect in the magnetic field is due to the rise in power release but not the proposed EMHD interaction! This important conclusion is very different from the authors' initial intentions to use a magnetic field in the experiments.

3.4 Discussion on shock wave control mechanisms

A qualitative physical model is proposed in this section to explain the mechanism of shock wave control by surface arc discharge. The sketch of physical problem for modeling is shown in figure 12, and the phenomenon can be simplified as a 2-D problem. In order to generate an oblique shock wave, a wedge is placed at the lower wall surface in the cold supersonic flow duct. The arc discharge electrodes are mounted in front of the wedge. The surface arc discharge plasma is generated and blown downstream by the cold supersonic flow, which can be seen from figure 3. From the discharge picture in experiments, the arc

discharge plasma covers large areas in front of the wedge and we suppose that the height of arc discharge plasma is less than the height of wedge. Flow viscosity is disregarded, so the boundary layer effects can be neglected. Because we just deduce the qualitative change laws of oblique shock wave control by arc discharge, the parameters quantities are not set concretely in this physical model.

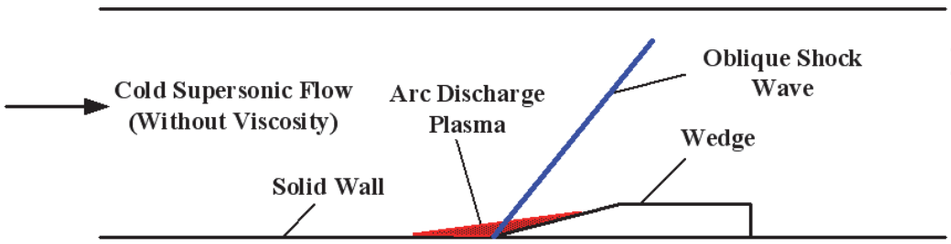

Fig. 12. Sketch of physical problem for modelling.

In the 1-D, steady and ideal gas flow, heating can accelerate the gas and decrease the gas pressure. As a result, the mass flux density of gas flow decreases, which is the mechanism of thermal choking phenomenon in the flow system. The influence of thermal choking effect on gas flow can be described as parameter

$$\varepsilon = \frac{\dot{m}_{\text{heat}}}{\dot{m}_{\text{unheat}}} = \frac{1}{\sqrt{1+\frac{s_0}{c_p T_0}}} \tag{1}$$

where ε is the ratio of mass flux density, $\dot{m}_{\text{heat}}$ and $\dot{m}_{\text{unheat}}$ are the mass flux density with and without gas heating respectively, s_0 is the amount of gas heating with unit mass, c_p and T_0 are the specific heat coefficient with constant pressure and gas static temperature without heating respectively, and $c_p T_0$ is the gas static enthalpy without heating. Defining nondimensional parameter $H_e = {s_0}/{c_p T_0}$ and it's the energy ratio of gas heating on initial static enthalpy with unit mass. Because $s_0 > 0$, $H_e > 0$ and $\varepsilon < 1$, which indicates that gas heating decreases the mass flux density of 1-D flow. When $H_e \to \infty$, $\varepsilon \to 0$, which indicates that if the amount of gas heating is extremely large, the mass flux density will decrease to zero and the gas flow will be totally choked. As arc discharge plasma can increase the gas temperature of cold supersonic flow from the level below 200 K to kilos of K rapidly, the amount of gas heating is very large, and the thermal choking phenomenon must be very remarkable in the flow duct.

Then we broaden the above 1-D analysis to the 2-D problem of shock wave control by arc discharge plasma. If the height of arc discharge plasma along the flow direction doesn't change, the flow area can be separated into two distinct regions with region *a* that corresponds to the cold supersonic flow area between arc discharge plasma and upper duct wall, and region *b* that corresponds to the high-temperature area of arc discharge plasma. The sketch is shown in figure 13. As the gas pressure of cold supersonic flow is about the high level of 10^4 Pa, arc discharge plasma often reaches the Local Thermal Equilibrium (LTE)

state approximately which indicates that the electron temperature equals to the ion and neutral gas temperature. Therefore, we can use one temperature to describe the thermal characteristics of arc discharge plasma.

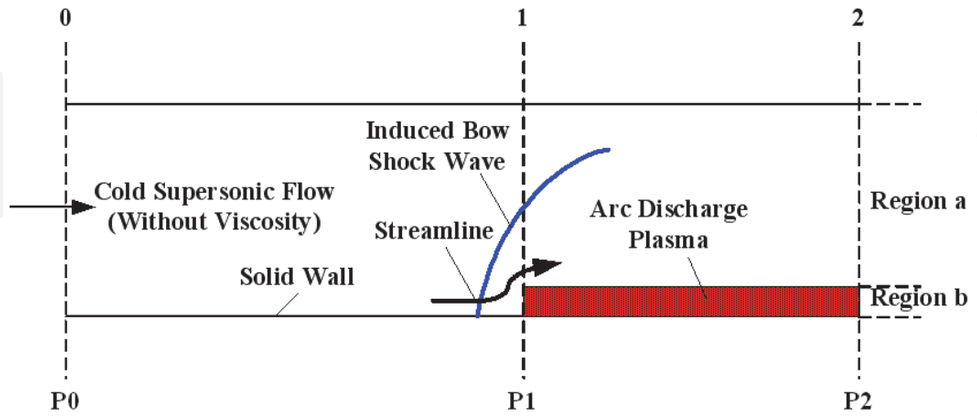

Fig. 13. Sketch of bow shock wave induction by arc discharge plasma.

When gas flows through the thermal area of arc discharge plasma, the mass flux will decrease because of thermal choking effect, then part of gas will pass to the cold gas flow area and the streamline will bend upward at section *1*. When the uniform flow reaches section 1, we suppose that the mass flux of region *a* and *b* will rearrange, so the 2-D problem is reduced to 1-D again after the flow passing through section 1. The gas pressure at the cross section of region *a* and *b* reaches equilibrium. Based on the above hypothesis, the mass flux density of region *a* and *b* can be described as

$$\dot{m}_a = \sqrt{\frac{(P_0 - P_2)P_2}{RT_{\text{a,unheat}}}} \tag{2}$$

$$\dot{m}_b = \sqrt{\frac{(P_0 - P_2)P_2}{RT_{\text{b,heat}}}} \tag{3}$$

where $\dot{m}_a$ and $\dot{m}_b$ are the mass flux density of region *a* and *b* respectively, P_0 and P_2 are the gas pressure of section *0* and *2* respectively, $T_{\text{a,unheat}}$ and $T_{\text{b,heat}}$ are the gas temperature of region *a* and *b* respectively and *R* is the universal gas constant. From equation (2) and (3), the mass flux density ratio of two regions is

$$\frac{\dot{m}_a}{\dot{m}_b} = \sqrt{\frac{T_{\text{b,heat}}}{T_{\text{a,unheat}}}} \tag{4}$$

So the mass flux ratio of two regions is

$$\frac{\dot{M}_a}{\dot{M}_b} = \frac{A_a}{A_b}\sqrt{\frac{T_{\text{b,heat}}}{T_{\text{a,unheat}}}} \tag{5}$$

where A_a and A_b are the cross section area of region *a* and *b* respectively, $\dot{M}_a$ and $\dot{M}_b$ are the mass flux of region *a* and *b* respectively.

Supposing the height of region *a* and *b* are 30mm and 2mm, respectively, so $A_a/A_b = 15$. In our experiments, the Mach number and gas stagnation temperature of the cold supersonic flow are 2.2 and 300 K, respectively. From the gas stagnation-static temperature equation

$$T^* = T\left(1 + \frac{\gamma+1}{2}M^2\right) \tag{6}$$

The gas static temperature is about 152 K, so $T_{\mathrm{a,unheat}} = 152K$. From the measurement in reference [8], the temperature of arc discharge plasma in the above cold supersonic flow can be estimated as 3000 K, so $T_{\mathrm{b,heat}} = 3000K$. Then $\dot{M}_a/\dot{M}_b \approx 67$ is acquired, which indicates that when cold supersonic gas meets the arc discharge plasma area, only little gas passes through the thermal area and most of the gas passes to the cold area. Therefore, we can conclude that the arc discharge plasma area can be regarded as a solid obstacle approximately and the gas flow cannot pass through it. Because the height of arc discharge plasma area is set constant in figure 6, the plasma area can be regarded as a rectangular blunt obstacle, which will induce a bow shock wave in the supersonic flow. However, in real conditions, the arc discharge plasma is streamlined by flow and the height of arc discharge plasma area increases from zero to larger value gradually, so the plasma area seems as a solid wedge, which can be called 'plasma wedge'. As a result, the plasma wedge will induce an oblique shock wave instead of a bow shock wave, which is shown in figure 14.

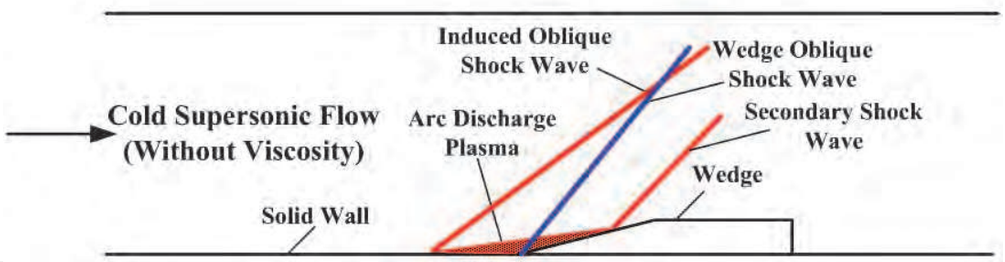

Fig. 14. Sketch of oblique shock wave control by arc discharge plasma.

Based on the above judgment of new shock wave induction by arc discharge plasma in cold supersonic flow, the wedge oblique shock wave control by arc discharge plasma is discussed as follows, which can be seen from figure 14. The wedge angle is designated as θ . Without arc discharge, the angle and intensity of wedge oblique shock wave are designated as β and π_s , respectively. After arc discharge, the plasma wedge will induce a new oblique shock wave in front of it and the old wedge oblique shock wave will disappear. Because the height of plasma wedge is less than the height of solid wedge, there is a secondary shock wave formed at the intersection point of plasma wedge and solid wedge. The plasma wedge angle is designated as θ^* . The angle and intensity of the induced oblique shock wave are designated as β^* and $\pi_s{}^*$, respectively. As $\theta^* < \theta$ and on the condition of constant Mach number, the relationships of $\beta^* < \beta$ and $\pi_s{}^* < \pi_s$ can be concluded based on the oblique shock wave relations of $(Ma \sim \theta \sim \beta)$.

Therefore, based on the above thermal choking model, we can conclude that the change laws of oblique shock wave control by arc discharge plasma are (1) the start point of shock wave will shift upstream, (2) the shock wave angle will decrease and (3) the shock wave intensity will weaken. The deduced theoretical result is consistent with the experimental result which demonstrates that the thermal choking model is rational to explain the problem of shock wave control by surface arc discharge.

4. Numerical simulation

Based on thermal mechanism, the arc discharge plasma is simplified as a thermal source term and added to the Navier-Stokes equations. The nonlinear partial difference equations are solved in ANSYS FLUENT® software. The flow modelling software is a widely used powerful computational fluid dynamics program based on finite volume method. It contains the broad physical modelling capabilities to model flow, turbulence, heat transfer, and reactions for industrial applications. It has excellent ability to simulate compressible flows. A user-defined function written in the C programming language is developed to define the thermal source term. The thermal source term uses the form of temperature distribution. The geometric shape of thermal source areas is supposed as rectangular and the gas temperature is uniform (3000 K). 2D coupled implicit difference method and k-epsilon two-equation turbulence models are used. The inlet flow conditions are consistent with the test conditions. As shown in figure 15, the width and height of rectangular thermal source area are 2 and 1 mm, respectively. According to the test condition of three pairs of electrodes discharging simultaneously, there are three pairs of thermal source areas with interval 2 mm.

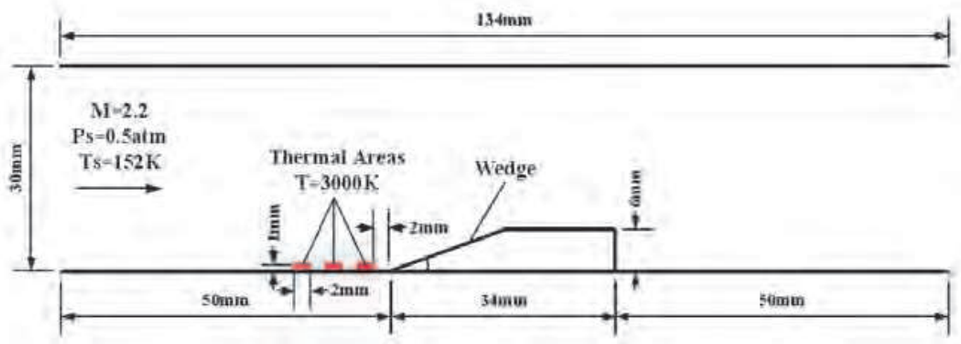

Fig. 15. Sketch of the numerical model.

As shown in figure 16(a), an oblique shock wave generates in front of the wedge, which matches the experimental results. After thermal energy addition to the supersonic flow field, we can see that the rectangular thermal source areas are blown downstream by the supersonic flow, which is shown in figure 16(b). It is consistent with the actual arc discharge picture in experiments. The geometric shape of the thermal area looks like a new wedge in front of the solid wedge and it is similar to the plasma wedge in the theoretical analysis. The influence of thermal energy addition on the wedge oblique shock wave is shown in figure 16(c). We can see that the start point of shock wave shifts upstream to the new wedge apex point and the shock wave angle decreases. The comparison curves of shock wave intensity are shown in figure 16(d), and we can see that the shock wave intensity decreases. These changes in shock wave are consistent with the experimental and theoretical results, which

demonstrate that the numerical method is reasonable. Also the thermal mechanism and thermal choking model are both validated.

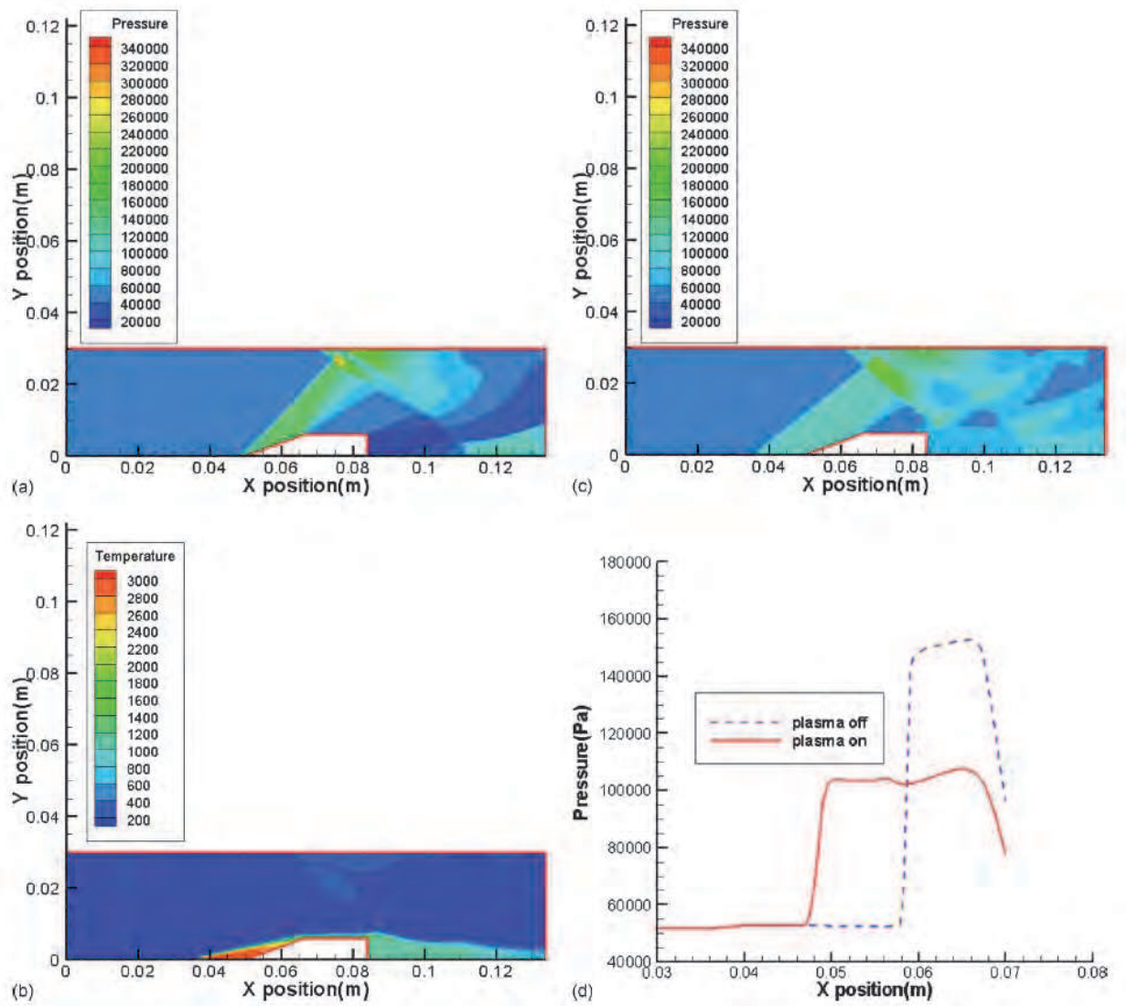

Fig. 16. Simulation results of oblique shock wave control by thermal energy addition. (a) Static pressure (Pa) contours without thermal energy addition. (b) Static temperature (K) contours with thermal energy addition. (c) Static pressure (Pa) contours with thermal energy addition. (d) Comparison curves of gas pressures along the centreline flow direction.

5. Conclusion

The wind tunnel experimental results demonstrate that the arc discharge plasma aerodynamic actuation controls the wedge oblique shock wave effectively, which shifts the start point of shock wave upstream, decreases the shock wave angle and weakens the shock wave intensity. Moreover, when applying magnetic control, the above shock wave control effect is greatly intensified. Under the typical plasma aerodynamic actuation conditions, the start point of the shock wave shifts 4 mm upstream, the shock wave angle decreases by 8.6% and its intensity weakens by 8.8%. Then the thermal choking model is proposed to explain

the thermal mechanism of shock wave control by plasma aerodynamic actuation. As the arc discharge adds substantial thermal energy to the cold supersonic flow field, the plasma area can be seen as a solid obstacle, which is called the 'plasma wedge'. Then the shock wave angle and the intensity change. The change laws of shock wave deduced by the thermal choking model are consistent with the experimental results, which demonstrate that the thermal choking model can effectively forecast the plasma actuation effects on a shock wave in a cold supersonic flow. Based on thermal mechanism, the arc discharge plasma was simplified as a thermal source term that added to the Navier-Stokes equations. The simulation results of the change in oblique shock wave were consistent with the test results, so the thermal mechanism indeed dominates the oblique shock wave control process.

6. References

Meyer, R., Palm, P. & Plonjes, E. (2001). The Effect of a Nonequilibrium RF Discharge Plasma on a Conical Shock Wave in a M=2.5 Flow, *32nd AIAA Plasmadynamics and Lasers Conference*, pp. 2-10, Anaheim, CA, USA, June 11-14, 2001

Merriman, S., Plonjes, E. & Palm, P. (2001). Shock Wave Control by Nonequilibrium Plasmas in Cold Supersonic Gas Flows, *AIAA Journal,* Vol.39, No.8, (August 2001), pp. 1547-1552, ISSN 0001-1452

Miles, R., Macheret, S. & Martinelli, L. (2001). Plasma Control of Shock Waves in Aerodynamics and Sonic Boom Mitigation, *32nd AIAA Plasmadynamics and Lasers Conference*, pp. 1-8, Anaheim, CA, USA, June 11-14, 2001

Macheret, S., Shneider, M. & Miles, R. (2003). Scramjet Inlet Control by Off-body Energy Addition: a Virtual Cowl, *41st AIAA Aerospace Sciences Meeting and Exhibit*, pp. 1-15, Reno, Nevada, USA, January 6-9, 2003

Shneider, M., Macheret, S. & Miles, R. (2003). Comparative Analysis of MHD and Plasma Methods of Scramjet Inlet Control, *41st AIAA Aerospace Sciences Meeting and Exhibit*, pp. 1-12, Reno, Nevada, USA, January 6-9, 2003

Leonov, S., Yarantsev, D. & Soloviev, V. (2006). High-speed Inlet Customization by Surface Electric Discharge, *44th AIAA Aerospace Sciences Meeting and Exhibit*, pp. 1-9, Reno, Nevada, USA, January 9-12, 2006

Leonov, S., Bityurin, V. & Yarantsev, D. (2005). High-speed Flow Control Due to Interaction with Electrical Discharges, *AIAA/CIRA 13th International Space Planes and Hypersonics Systems Technologies Conference*, pp. 1-12, Capua, Italy, May 16-20, 2005

Leonov, S., Yarantsev, D. & Isaenkov, Y. (2005). Properties of Filamentary Electrical Discharge in High-enthalpy Flow, *43rd AIAA Aerospace Sciences Meeting and Exhibit*, pp. 1-14, Reno, Nevada, USA, January 10-13, 2005

Kolesnichenko, Y., Brovkin, V. & Leonov, S. (2001). Investigation of AD-body Interaction with Microwave Discharge Region in Supersonic Flows, *39th AIAA Aerospace Sciences Meeting and Exhibit*, pp. 1-12, Reno, Nevada, USA, January 8-11, 2001

Bletzinger, P., Ganguly, B. & VanWie, D. (2005). Plasmas in High Speed Aerodynamics, *Journal of Physics D*： *Applied Physics,* Vol.38, No.4, (April 2005), pp. R33–57, ISSN 0022-3727

Ganiev, Y., Gordeev, V. & Krasilnikov, A. (2000). Aerodynamic Drag Reduction by Plasma and Hot-gas Injection, *Journal of Thermophysics and Heat Transfer,* Vol.14, No.1, (January-March 2000), pp. 10-17, ISSN 0887-8722

Shang, J. (2002). Plasma Injection for Hypersonic Blunt-body Drag Reduction, *AIAA Journal,* Vol.40, No.6, (June 2002), pp. 1178-1186, ISSN 0001-1452

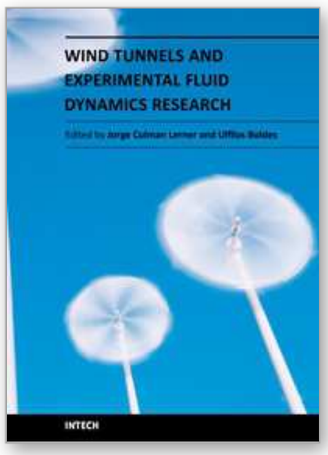

Wind Tunnels and Experimental Fluid Dynamics Research

Edited by Prof. Jorge Colman Lerner

ISBN 978-953-307-623-2
Hard cover, 709 pages
Publisher InTech
Published online 27, July, 2011
Published in print edition July, 2011

The book â€œWind Tunnels and Experimental Fluid Dynamics Researchâ€ is comprised of 33 chapters divided in five sections. The first 12 chapters discuss wind tunnel facilities and experiments in incompressible flow, while the next seven chapters deal with building dynamics, flow control and fluid mechanics. Third section of the book is dedicated to chapters discussing aerodynamic field measurements and real full scale analysis (chapters 20-22). Chapters in the last two sections deal with turbulent structure analysis (chapters 23-25) and wind tunnels in compressible flow (chapters 26-33). Contributions from a large number of international experts make this publication a highly valuable resource in wind tunnels and fluid dynamics field of research.

InTech Europe
University Campus STeP Ri
Slavka Krautzeka 83/A
51000 Rijeka, Croatia
Phone: +385 (51) 770 447
Fax: +385 (51) 686 166
www.intechopen.com

InTech China
Unit 405, Office Block, Hotel Equatorial Shanghai
No.65, Yan An Road (West), Shanghai, 200040, China
中国上海市延安西路65号上海国际贵都大饭店办公楼405单元
Phone: +86-21-62489820
Fax: +86-21-62489821

IntechOpen